Eur. Phys. J. D **24**, 257–260 (2003)
DOI: 10.1140/epjd/e2003-00101-2

THE EUROPEAN PHYSICAL JOURNAL D

Core size effects on electrodeposition of gold nanoparticles attached with biferrocene derivatives

M. Yamada and H. Nishihara[a]

Department of Chemistry, School of Science, The University of Tokyo, Tokyo 113-0033, Japan

Received 10 September 2002
Published online 3 July 2003 –

Abstract. Biferrocene-modified gold nanoparticles (Au_n-BFc) comprising 1.7, 2.2 and 2.9 nm in average core diameter, d, were synthesized by a substitution reaction of octyl thiolate-covered nanoparticles with biferrocene-terminated alkanethiol, 1-(9-thiononyl-1-one)-1′, 1″-biferrocene (BFcS). All sizes of Au_n-BFc undergo two-step oxidation reactions in 0.1 mol dm^{-3} Bu_4NClO_4-CH_2Cl_2 and consecutive potential scans including the second oxidation process lead to the formation of an adhesive redox-active gold nanoparticle film on an electrode. The thickness of the Au_n-BFc film is controllable by the number of potential scans. The scanning tunneling microscope images reveal that the Au_n-BFc ($d = 2.9$ nm) film forms many domains of the assembled Au_n-BFcs, especially the particles are isotropically assembled in line.

PACS. 73.22.-f Electronic structure of nanoscale materials: clusters, nanoparticles, nanotubes, and nanocrystals

1 Introduction

Since Brust *et al.* reported the simple and easy synthetic method of alkylthiolate-covered gold nanoparticles with narrow polydispersities in core diameter [1], enormous following researches have been performed *e.g.* the synthetic variations [2–5], high-dimensional construction on a substrate [6–9], characteristic features [10–13], and theoretical calculations [14–16]. In order to produce novel nano-sized materials by combining the unique electrochemical and optical properties of metal nanoparticles with functional molecules with redox or photo-active species, we previously introduced biferrocene (BFc) [17,18], anthraquinone (AQ) [19,20], and porphyrin [21], onto the surface of metal nanoparticles by ligand exchange reactions between the functional molecules and metal nanoparticles stabilized by alkyl ligands [22,23]. There we found that the functionalized metal nanoparticles built up the multilayered nanoparticle films on the substrate triggered by outside simulation mainly due to introduced molecules; for instance, oxidation of the BFc units-attached gold nanoparticles (Au_n-BFc) affords the multilayered films when the BFc units become the biferrocenium(2+) state. This deposition system not only provokes a fundamental interest in aggregation mechanism of colloidal particles, but also will provide a new methodology for constructing three-dimensional networks of metal nanoparticles. Our previous study on the mechanism of Au_n-BFc electrochemical deposition has suggested that the highly charged Au_n-BFc^{2+} in electrolyte-CH_2Cl_2 solution eliminates the solvents around the particles, which causes the inter-particle interaction *via* electrolyte anions [24], although the reason why the particles are being aggregated in the film even when the BFc sites are in the neutral form has not been fully clarified. The inter-particle interaction, which plays an important role in the aggregation process, should include the van der Waals force, depending on the nanoparticle size. In the present study, we thus synthesized three samples of Au_n-BFc particles with different average core diameters, and investigated the dependence of Au_n-BFc electrodeposition on the core size. Observation of the Au_n-BFc film by scanning tunneling microscope (STM) gave an interesting morphological feature.

2 Experimental section

All reagents were of extra-pure grade, and were purchased from Kanto Chemicals or Tokyo Kasei. They were used as received, unless otherwise noted. All organic solvents were of HPLC grade (Kanto Chemicals). Tetra-*n*-butylammonium perchlorate (Bu_4NClO_4) was used after recrystallization from ethanol. The preparation of Au_n-BFc (**1**, **2**, and **3**) with a different core diameter was performed based on our previous papers summarized in Figure 1 [17]. They were prepared by 1:4 mole feed ratio of BFcS to octyl thiolate units on the particle surface of the octyl thiolate-covered gold nanoparticles (Au_n-OT) in substitution reaction in CH_2Cl_2 for 2 days. Three samples of Au_n-OT with a different core diameter were prepared by the Brust's method [1] with changing the feed mole ratio of $AuCl_4^-$ to octanethiol (1 to 2 for **1**, 1 to 1 for **2**, and 4 to 1 for **3**) in synthetic condition [25].

[a] e-mail: nisihara@chem.s.u-tokyo.ac.jp

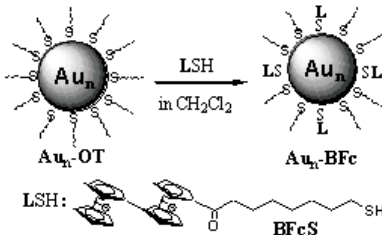

Fig. 1. Preparation of Au_n-BFc.

The ^{1}H-NMR spectra of the samples in $CDCl_3$ were collected with a JEOL EX270 spectrometer. UV-vis absorption spectra were recorded with an Agilent 8453 UV-visible Spectroscopy System. TEM images of Au_n-BFc were obtained with a Hitachi HF-2000 microscope. Samples for TEM were prepared by drop-casting 4 ml of a 0.5 mg/ml Au_n-BFc solution in CH_2Cl_2 onto standard carbon-coated films on copper grids (600 mesh, from Ohta Giken) and drying them under vacuum overnight. Size distribution of the metal cores was measured from enlarged TEM images for at least 200 individual particles using the computer program Scion Image Release 4 (Scion Corporation). Electrodeposition of Au_n-BFc on an indium-tin oxide (ITO)-coated glass electrode (1.0×1.5 cm^2) was carried out with consecutive scans between -0.3 and 0.9 V *vs.* Ag/Ag^+ [10 mmol dm^{-3} $AgClO_4$ in 0.1 M Bu_4NClO_4-MeCN, $E^{0'}(Fc/Fc^+) = 0.27$ V *vs.* Ag/Ag^+ (Fc: ferrocene)] in a solution of Au_n-BFc in 0.1 mol dm^{-3} Bu_4NClO_4-CH_2Cl_2 at room temperature using a platinum-wire counter electrode. The ITO electrodes were washed in ultra pure water (>18.2 MΩ cm^{-1}) containing a protein remover for 5 min and cleaned by ultra pure water and acetone for 5 min, respectively, under sonication before the experiment. The electrodeposited films were sufficiently cleaned with CH_2Cl_2 after the preparation process then dried under vacuum over night. STM topographic images of the electrodeposited film on HOPG were taken at a constant current of 0.3−0.5 nA and a bias of 0.1−0.5 V with a Pt/Ir (4:1) tip with a PicoSPM (Molecular Imaging) controlled by a PicoScan (Molecular Imaging) at room temperature in air.

3 Synthesis and electrodeposition of Au_n-BFc

Au_n-OT particles were prepared by the Brust method, using reduction of $HAuCl_4$ with a 10-fold excess of $NaBH_4$ in the presence of octanethiol in single organic phase [1]. The average core diameter of Au_n-OT thus prepared was determined by TEM to be 1.7 ± 0.5 nm for **1**, 2.2 ± 0.5 nm for **2**, and 2.9 ± 0.8 nm for **3**, indicating that the high ratio of $HAuCl_4$ to octanethiol gave a larger nanoparticle size and a large standard deviation in good agreement with the literature [25]. While the UV-vis spectrum of **2** and **3** in CH_2Cl_2 exhibits a surface plasmon (SP) band [14] at 510 nm ($\varepsilon_{max} = 7.7 \times 10^5$ mol^{-1} dm^3 cm^{-1}, and $\varepsilon_{max} = 2.4 \times 10^6$ mol^{-1} dm^3 cm^{-1}, respectively), that of **1** only shows a gentle curve attributed to the Mie scattering (Fig. 2, inset). The loss of the SP band in **1** is

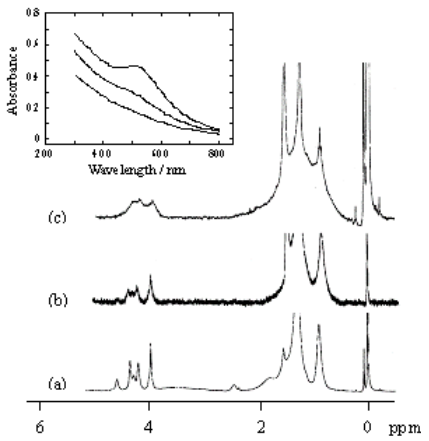

Fig. 2. ^{1}H-NMR spectra of compound **1** (a), **2** (b), and **3** (c). (inset) UV-vis spectra in toluene of **1** ($C = 5.6 \times 10^{-7}$ mol dm^{-3}), **2** ($C = 4.6 \times 10^{-7}$ mol dm^{-3}), and **3** ($C = 2.0 \times 10^{-7}$ mol dm^{-3}), as shown from the bottm of the figure to the top.

Table 1. Size and composition of Au_n-BFc's.

Au_n-BFc	Core diameter / nm	Number of Au atoms	Number of thiolates on the surface	θ_{BFc}
1	1.7 ± 0.5	201	71	4.7
2	2.2 ± 0.5	309	92	7.5
3	2.9 ± 0.8	976	187	20.8

interpreted as the indication of the onset of quantum size effects and the loss of bulk character for the smaller gold core [25]. The number of exchanged BFcS on the Au_n-OT surface, θ_{BFc}, was calculated by the ratio of the integrals of the ^{1}H-NMR signals between BFc and methyl protons at 3.9−4.7 ppm and 0.8−0.9 ppm, respectively. Figure 2 shows that the ^{1}H-NMR signal of Au_n-BFc with a larger core diameter is broadened more significantly, suggesting that dipolar spin relaxation caused by the dense chain packing on the nanoparticle surface works more effectively for larger particle size. Size and composition data [26] for **1**, **2**, and **3** are summarized in Table 1.

Figure 3A shows the typical cyclic voltammograms of Au_n-BFc in the electrodeposition process, which is measured in a solution of **3** at ITO in 0.1 mol dm^{-3} Bu_4NClO_4-CH_2Cl_2 between -0.3 and 0.9 V *vs.* Ag/Ag^+. The two-step one-electron oxidation due to BFc units on a gold nanoparticle surface occurs at $E_1^{0'} = 0.20$ and $E_2^{0'} = 0.61$ V *vs.* Ag/Ag^+ at the first scan. The peak current increases gradually by consecutive potential scans and the cathodic peak current is larger than the anodic peak current especially observed at the first scan, suggesting the formation of an adhesive Au_n-BFc film on ITO. The redox potential of the BFc moieties of **3** becomes slightly shifted in the negative direction at $E_1^{0'} = 0.19$ V and $E_2^{0'} = 0.60$ V when the electrodeposition proceeds, effected by the assembled Au_n-BFc particles strongly attached to the electrode in addition to the diffusive

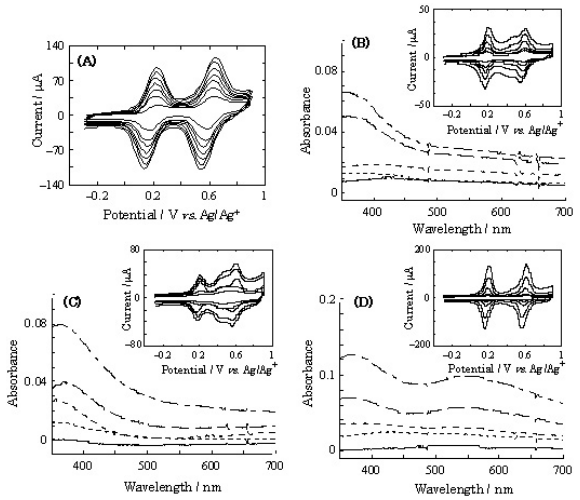

Fig. 3. (A) Cyclic voltammograms at the 1st, 10th, 20th, 30th, 40th, 50th, and 60th cyclic scans, as shown from the bottom of the figure to the top, during electrodeposition of **3** (1.7 mmol dm^{-3}) at ITO by consecutive potential scans between −0.3 to 0.9 V *vs.* Ag/Ag$^+$ in 0.1 M Bu_4NClO_4–CH_2Cl_2 at 100 mV s^{-1}. (B, C, D) UV-vis spectra of electrodeposited Au_n-BFc films prepared in solutions of 8.0 μmol dm^{-3} of **1**, 5.0 μmol dm^{-3} of **2**, and 1.7 μmol dm^{-3} of **3**, respectively, in 0.1 mol dm^{-3} Bu_4NClO_4–CH_2Cl_2 at 100 mV s^{-1} between −0.3 to 0.9 V *vs.* Ag/Ag$^+$ for 3, 10, 25, 50, and 75 cyclic scans, as shown from the bottom of the figure to the top. (Inset of B, C and D) Cyclic voltammograms of the films prepared as above in 0.1 mol dm^{-3} Bu_4NClO_4–CH_2Cl_2.

Au_n-BFc particles in solution. UV-vis spectra of the Au_n-BFc film of **1**, **2**, and **3** deposited in the same way described above exhibit broad absorption bands that grow in intensity with increase in the number of potential scans (Figs. 3B, 3C, and 3D), indicating that the construction of gold nanoparticle films with a different core diameter is applicable by using this electrodeposition process. Thickness of the film can be controlled by changing the number of potential scans. The coverage of Au_n-BFc onto the electrode increases almost proportionally to the number of scans, considering the correlation between the intensity of the film at 510 nm of the SP band and the number of scans. By using the absorption intensity of the film and the molar extinction coefficient of Au_n-BFc, the coverage of the thickest Au_n-BFc film prepared with 75 scans is calculated to be 8.2×10^{-11} mol cm^{-2} for **1**, 3.6×10^{-11} mol cm^{-2} for **2**, and 3.9×10^{-11} mol cm^{-2} for **3**, respectively. These values are not largely different, but following experiments are needed to discuss further whether the smaller or larger core size is more effective for the electrodeposition since the values of θ_{BFc}, which is one important parameter for rate of electrodepsiton, are not consistent to each other (Tab. 1). The values of the coverage correspond to 7−13 Au_n-BFc layers with 40−60 nm thickness assuming that the electrodeposited Au_n-BFcs in the film are closely packed with a spacing of estimated maximal diameter (core diameter $d = 1.7$, 2.2 or 2.9 nm; octyl thiolate, 1.0 nm; and BFc unit, 0.8 nm). Cyclic voltammetry of the Au_n-BFc film shows two of each cathodic and anodic waves of which the peak-to-peak separation is *ca.* 10 mV for the thin film (Figs. 3B, 3C, and 3D, inset) attributed to the immobilized BFc species of the film. The peak-to-peak separation becomes larger with increases in the film thickness by the fact that film resistance prevents the electron transfer among the particles in the film. These results show that electrodeposition of Au_n-BFc proceeds successfully by the same way of two-electron oxidation of BFc units on the particle surface, independent of the core size; however, it should be noted that the following two obvious remarks are observed by comparing three different samples: (i) only the Au_n-BFc film of **3** exhibits the broad absorption band at *ca.* 550 nm, and (ii) do not show additional redox wave at *ca.* 0.4 V which appears between the original redox waves of BFc units. The broad absorption band is due to the collective SP band influenced by the dipole-dipole coupling among the adjacent particles [27], suggesting that the inter-particle interaction among larger particles which have the strong SP resonance originally, leading to display stronger collective bands. The newly appeared redox wave originates from the decomposition of BFc units in the electrodeposited film on the electrode caused by oxidative forms of BFc units [28]. It is plausible that the conductivity in the Au_n-BFc film of **3** is relatively high with a large ratio of metal part in volume, resulting in efficient electron transfer among Au_n-BFc particles in the film that prevents the decomposition of BFc species. This lessens the contribution of the redox conduction process between two BFc sites, which would be a significant cause of the intermolecular decomposition reaction.

4 STM images of the electrodeposited Au_n-BFc films

We investigated the morphological features of the electrodeposited Au_n-BFc film and the changes in the surface structure by varying the core size. Figure 4 demonstrates an STM image of the Au_n-BFc film of the largest particle, **3** on HOPG electrodeposited in 0.1 mol dm^{-3} Bu_4NClO_4–CH_2Cl_2 by 5 potential scans. At this small number of scans, heterogeneous morphology, showing islands of particles can be recognized. This is similar to the image of smaller nanoparticeles, **2** [24], suggesting that Au_n-BFcs tend to assemble voluntarily in this film formation process. In Figure 4A, some particles which form an isotropic assembly in line are shown. The distance between the particles in line is 7.5 nm, and that between the lines is 13 nm, which agrees with the electrodeposition mechanism based on inter-particle interaction. We observed that Au_n-AQ film [19] which tends to gather in the tetragonal array structure in the early stage of electrodeposition. These findings mean that some equilibrium in the collective interaction among the aggregated particles exists to display a regular construction of particles in the film, and give hints on the methodology of dimensionally-ordered nanoparticle array fabrication by the electrochemical deposition technique.

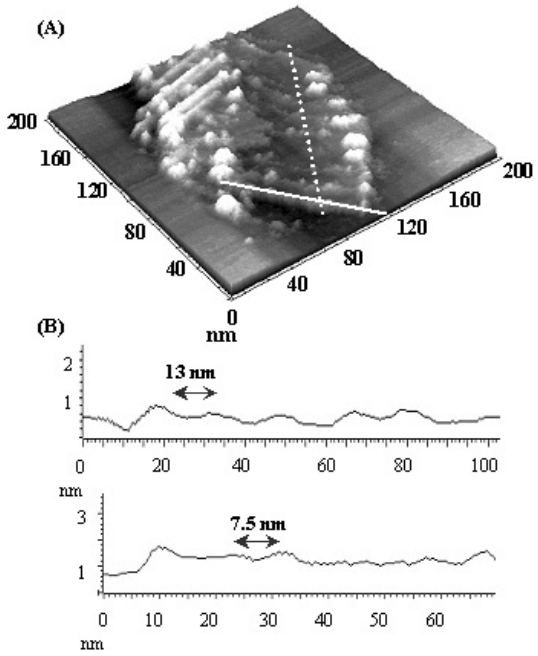

Fig. 4. (A) STM images of an Au_n-BFc film on HOPG electrodeposited in a solution of 1.7 mmol dm^{-3} of **3** in 0.1 mol dm^{-3} Bu_4NClO_4–CH_2Cl_2 between −0.3 and 0.9 V *vs.* Ag/Ag^+ at 100 mV s^{-1} by 5 cyclic scans with the cross-sectional profiles along the dotted (B, top) and the solid (B, bottom) line.

5 Conclusion

We have presented a novel method to fabricate octylthiolate-covered gold nanoparticle films with a various core diameter by using electro-oxidative process of the biferrocene units introduced onto the particle surface. The electrodeposited films possess a unique morphological feature convinced by STM observation.

This work was supported by Grant-in-Aid for Scientific Research (No. 14204066) from the Ministry of Culture, Education, Science, Sports, and Technology, Japan, and the Research Fellowships of the Japan Society for the Promotion of Science for Young Scientists.

References

1. M. Brust, M. Walker, D. Bethell, D.J. Shiffrin, R. Whyman, J. Chem. Soc., Chem. Commun. 801 (1994)
2. I. Quiros, M. Yamada, K. Kubo, J. Mizutani, M. Kurihara, H. Nishihara, Langmuir **18**, 1413 (2002)
3. Y.S. Shon, G.B. Dawson, M. Porter, R.W. Murray, Langmuir **18**, 3880 (2002)
4. R. Blonder, L. Sheeney, I. Willner, Chem. Commun. 1393 (1998)
5. D. Gerion, F. Pinaud, S.C. Williams, W.J. Parak, D. Zanchet, S. Weiss, A.P. Alivisatos, J. Phys. Chem. B **105**, 8861 (2001)
6. Y. Men, K. Kubo, M. Kurihara, H. Nishihara, Phys. Chem. Chem. Phys. **3**, 3377 (2001)
7. S. Murthy, Z.L. Wang, R.L. Whetten, Phil. Mag. Lett. 321 (1997)
8. M.M. Maye, Y.B. Lou, C.J. Zhong, Langmuir **16**, 7520 (2000)
9. C.J. Kiely, J. Fink, M. Brust, D. Bethell, D.J. Schiffrin, Nature **396**, 444 (1998)
10. T. Sagara, N. Kato, N. Kakashima, J. Phys. Chem. B **106**, 1205 (2002)
11. T. Huang, R.W. Murray, J. Phys. Chem. B **105**, 12498 (2001)
12. S. Pethkar, M. Aslam, I.S. Mulla, P. Ganeshan, K. Vijayamohanan, J. Mater. Chem. **11**, 1710 (2001)
13. T.P. Bigioni, L.E. Harrell, W.G. Cullen, D.E. Guthrie, R.L. Whetten, P.N. First, Eur. Phys. J. D **6**, 355 (1999)
14. P. Mulvaney, Langmuir **12**, 788 (1996)
15. S.W. Chen, R.W. Murray, S.W. Feldberg, J. Phys. Chem. B **102**, 9898 (1998)
16. N. Pincon, B. Palpant, D. Prot, E. Charron, S. Debrus, Eur. Phys J. D **19**, 395 (2002)
17. T. Horikoshi, M. Itoh, M. Kurihara, K. Kubo, H. Nishihara, J. Electroanal. Chem. **113**, 473 (1999)
18. M. Yamada, I. Quiros, J. Mizutani, K. Kubo, H. Nishihara, Phys. Chem. Chem. Phys. **3**, 3377 (2001)
19. M. Yamada, T. Tadera, K. Kubo, H. Nishihara, Langmuir **17**, 2363 (2001)
20. M. Yamada, K. Kubo, H. Nishihara, Chem. Lett. 1335 (1999)
21. M. Yamada, A. Kuzume, M. Kurihara, K. Kubo, H. Nishihara, Chem. Commun. 2476 (2001)
22. M.J. Hostetler, S.J. Green, J.J. Stokes, R.W. Murray, J. Am. Chem. Soc. **118**, 4212 (1996)
23. A. Labande, J. Ruiz, D. Astruc, J. Am. Chem. Soc. **124**, 1782 (2002)
24. M. Yamada, T. Tadera, K. Kubo, H. Nishihara, J. Phys. Chem. B (in press, 2003)
25. M.J. Hostetler, J.E. Wingate, C.-J. Zhong, J.E. Harris, R W. Vachet, M.R. Clark, J.D. Londono, S.J. Green, J.J. Stokes, G.D. Wignall, G.L. Glish, M.D. Porter, N.D. Evans, R.W. Murray, Langmuir **14**, 17 (1998)
26. M.M. Alvarez, J.T. Khoury, T.G. Schaaff, M.N. Shafigullin, I. Vezmar, R.L. Whetten, J. Phys. Chem. B **101**, 3706 (1997)
27. T. Ung, L.M. Liz-Marzan, P. Mulvaney, J. Phys. Chem. B **105**, 3441 (2001)
28. K. Kubo, H. Kondow, H. Nishihara, Electrochemistry **67**, 1129 (1999)